THE SABrR CONCEPT FOR A FISSION-FUSION HYBRID ^{238}U-TO-^{239}PU FISSILE PRODUCTION REACTOR

FISSION REACTORS

KEYWORDS: *fission-fusion hybrid, fast breeder reactor, subcritical*

C. L. STEWART* and W. M. STACEY

Georgia Institute of Technology, Nuclear & Radiological Engineering Program
Fast Reactor Research Group

Received July 4, 2013
Accepted for Publication August 30, 2013
http://dx.doi.org/10.13182/NT13-102

The subcritical advanced burner reactor (SABR) concept, which combines IFR-PRISM fast reactor technology and the ITER tokamak fusion physics and technology in a burner reactor for the transmutation of transuranics, has been adapted for a subcritical advanced breeder reactor (SABrR) that produces plutonium. It is found that basically the same fission and fusion technology, geometry, and major parameters as used in SABR can be used to achieve a significant fissile production rate (fissile breeding ratio ≈ 1.3) while maintaining tritium self-sufficiency (tritium breeding ratio >1.15).

Note: Some figures in this paper may be in color only in the electronic version.

I. INTRODUCTION

Closing the nuclear fuel cycle is an important step in advancing the prospect of nuclear energy in both the near and far terms. The once-through cycle largely employed today uses a very small percentage of the potential energy content of natural uranium and produces high-level waste, for which we have yet to implement a long-term solution. A solution to the overall fuel cycle problem would have the dual benefits of extending the uranium resources of Earth by a factor of 10 to 100 over the once-through cycle and of greatly reducing the volume, decay heat, and longevity of repository-bound waste. Various fast reactor technologies and designs have been developed with the intent of closing the front end[1,2] (breeder reactors), the back end[3–5] (burner reactors), or both.[6–8]

Breeder reactors take advantage of the high neutron-per-fission yield of fissile isotopes, particularly ^{239}Pu, in fast neutron spectra to supply extra neutrons beyond those necessary to sustain the fission chain reaction. These excess neutrons are captured in fertile material such that more fissile material is produced than was consumed. Burner reactors leverage a fast neutron spectrum to transmute, preferably by fission, transuranic (TRU) isotopes that remain in the spent fuel discharged from thermal reactors. These TRUs, which constitute a substantial fraction[4] (tens of percent) of burner reactor fuel, would otherwise be sent directly to a geological repository and dominate the long-term radiotoxicity and decay heat of the used nuclear fuel.[9,10] Some reactor designs[6–8] incorporate the aspects of both breeders and burners. They are intended to operate in an integrated fuel cycle, mixing their own discharged fuel with used fuel from other reactors and depleted uranium to form the next fuel loading. One of the most mature of these integrated reactor concepts is the integral fast reactor[6,7,11] (IFR); many of its design decisions and material choices reflect its integrated fuel cycle and the very hard neutron spectrum which that cycle requires.

A subcritical advanced burner reactor (SABR) concept that addresses the waste problem is being developed at the Georgia Institute of Technology.[12,13] SABR is a sodium-cooled, 3000 MW(thermal) annular fast reactor consisting of four assembly rings surrounding a toroidal plasma. The fission core operates in the

*E-mail: cstewart37@gatech.edu

subcritical regime; the plasma supplies an external neutron source via the D-T fusion reaction. The fuel pins of SABR are loaded with TRUs processed from used fuel from light water reactors (LWRs) that is fissioned to a high atomic percent burnup. Neutrons leaking from the fission core are captured in surrounding tritium breeding blankets to produce fuel for the fusion reaction. Because of the subcritical operation, SABR is postulated to be able to be fueled with 100% TRU fuel discharge from LWRs, as contrasted with the tens of percent envisioned for critical reactors.[4] Fuel cycle calculations[14,15] indicate that SABR could consume TRUs at triple the rate that an LWR of the same power output produces them; a future reactor fleet might then produce 75% of its electricity in LWRs and 25% in SABRs and send no TRUs, other than losses from reprocessing, to repositories. SABR is based on existing technologies developed for the IFR and on ITER physics and technology and could be deployed by the midcentury.

Because the plasma and technology performance required for an economical fusion power plant significantly exceeds that which will be demonstrated in ITER, developing fission-fusion hybrid (FFH) reactors with ITER-level plasma and technology requirements in parallel with the further plasma and technology development needed for pure fusion power would allow for substantial accumulation of power reactor operating experience with tokamaks prior to the introduction of pure fusion power plants into reactor fleets.[13] In the near term, these FFHs would likely be devoted to burning actinides, while in the longer term, using them for fissile production becomes more desirable as easy-to-extract ^{235}U becomes depleted. The SABR studies indicate the efficacy of the FFH in the burner role. An important question then arises: Could a similar hybrid reactor make a useful contribution as a breeder?

Moir[16] and Moir et al.[17] have explored a FFH breeder in some depth, investigating economic scenarios and materials choices with respect to different fertile isotopes and LWR support ratios. Those studies focused on a tandem mirror fusion device with substantially different geometry than SABR. Nevertheless, the important considerations are the same as for a tokamak-geometry fast breeder FFH. A key challenge in designing an effective FFH breeder is the neutron economy: Of the neutrons released from each fission, somewhat less than one must go toward sustaining the chain reaction, a fraction are captured parasitically in fissile material and structural materials, a fraction leak out of the reactor, and the remainder are available for absorption in fertile material to breed fissile material and fuel for the fusion reaction.

The purpose of this paper is to investigate whether or not the basic SABR configuration and fusion physics and technology can be effectively used to breed fissile material. Instead of the TRU fuel used in the SABR burner reactor, the fuel pins for the subcritical advanced breeder reactor (SABrR) contain U-Pu-Zr and U-Zr metal fuel. The primary difference in neutronics design challenges between the burner and breeder SABRs revolves around the neutron economy. Whereas in the burner reactor, only the total fission rate and the tritium breeding ratio (TBR) are important, in the breeder reactor, both the TBR and the fissile breeding ratio (FBR) are important. Previous calculations indicate that a TBR $>$ 1.15 must be maintained to provide for tritium self-sufficiency of the fusion neutron source, and a FBR of significantly greater than unity must be achieved to provide fissile material for other reactors. The challenge of keeping a sufficiently high TBR in SABrR is exacerbated by the presence of U-Zr fissile breeding blankets between the annular fission core and the surrounding tritium breeding blanket, which significantly reduces the neutron flux incident on the tritium breeding blankets in the breeder relative to the burner. With this in mind, two configurations of the tritium blanket and reflector structures were considered: one that maximizes the TBR and one that maximizes the FBR.

Ultimately, any FFH design must compare favorably to critical fast fission reactor designs to justify the added cost and complexity of including the fusion element. Such a comparison must include comparative analyses of (a) the fissile production capability of subcritical and critical fast breeder reactors, (b) the dynamic responses of the subcritical and critical designs to various accident scenarios, (c) the overall cost and reliability of the system of breeder reactors and reprocessing/refabrication facilities, and (d) the resistance to proliferation. The first step in this evaluation is to establish a realistic subcritical (FFH) fast breeder reactor technology for comparison with critical fast breeder reactor concepts.

This paper establishes the core design of two variants of the SABrR geometry and evaluates their capability to breed fissile material within several constraints established for the SABR design[12]; future studies on the safety performance of SABrR will be based on this design. Although no effort has been made to optimize the fissile breeding performance of these initial SABrR designs within a particular fuel cycle, a comparison of breeding performance and fuel cycles is made with a critical high-breeding, metal-fueled S-PRISM core design to illustrate the feasibility of SABrR.

II. SABrR DESIGN CONCEPT

II.A. SABrR Design Overview

The top-level configuration of the SABR burner concept is shown in Fig. 1, and a detailed R-Z cross section is shown in Fig. 2. The entirety of the fusion and fission systems resides within the superconducting toroidal magnets of the tokamak. The inner edge of the

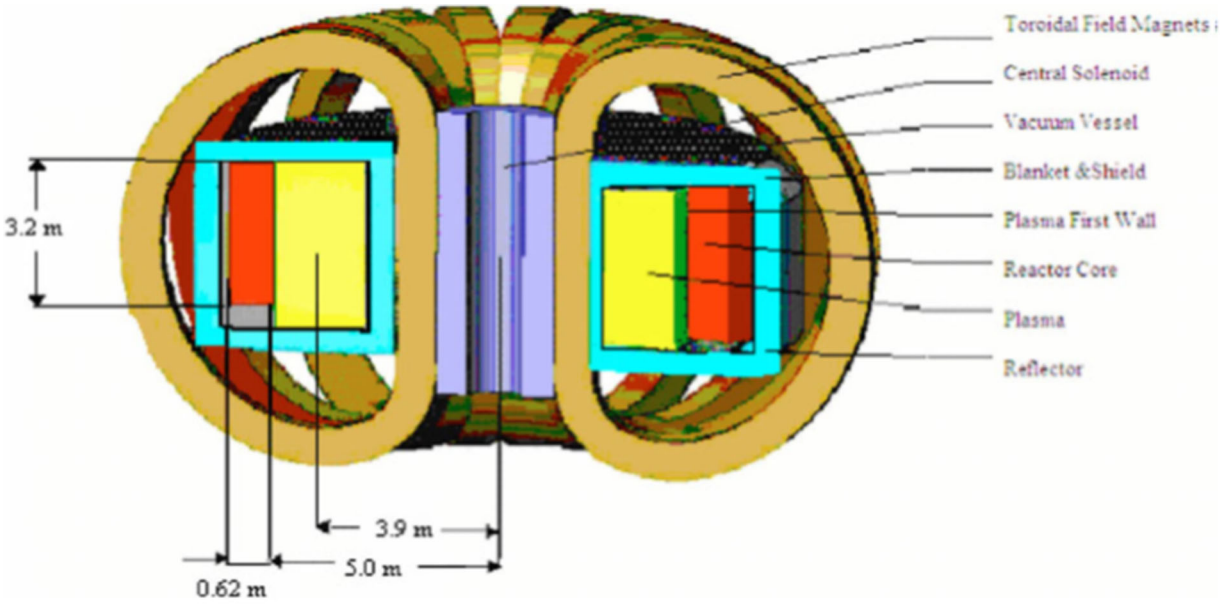

Fig. 1. SABR configuration.

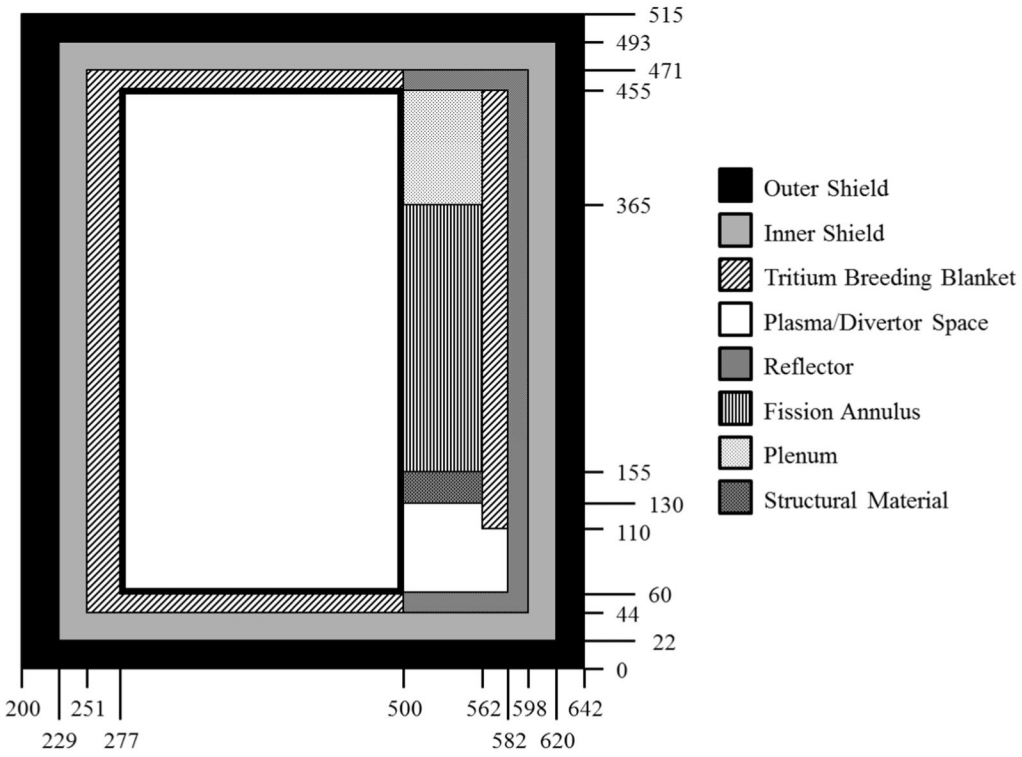

Fig. 2. R-Z cross section of SABR (dimensions in units of centimeters).

annular fission core lies at the outer edge of the tokamak plasma chamber wall. Surrounding the plasma chamber and fission core annulus are first the tritium breeding blankets and then the stainless steel reflector. Finally, these are enveloped by multilayer shields that reduce the fast neutron and gamma fluences to the

superconducting magnets, giving them a lifetime of at least 30 full-power years.

II.B. Fusion Neutron Source

The fusion neutron source is provided by a tokamak based on ITER physics and is capable of 500 MW of fusion power. Deuterium and tritium in the plasma undergo the reaction ${}_1^2\mathrm{D}+{}_1^3\mathrm{T}\rightarrow{}_2^4\mathrm{He}+{}_0^1n$. The helium nucleus will deposit most of its energy, $\sim$3.5 MeV, into the plasma. However, the neutron, carrying 14.1 MeV, will stream directly out of the plasma, since it has no charge and is therefore not bound by the magnetic fields confining the plasma. This neutron, possessing energy several times that of the average fission neutron, is extremely well-suited to sustaining a subcritical fission reaction: Not only is the fission-to-capture ratio for heavy metal nuclides higher at such high energies, but the neutron also has energy well in excess of the threshold fission reactions in the even-neutron isotopes, of which ^{238}U, ^{240}Pu, and ^{242}Pu are of primary importance. Furthermore, $(n,2n)$ and $(n,3n)$ reactions contribute substantially to neutron production via the fusion source due to the increase of these cross sections at high neutron energy.

It is not difficult to obtain half of the fuel for the D-T fusion reaction. Deuterium, present in about 1 of every 10 000 water molecules, is relatively easy to recover. Tritium, however, has a half-life of 12.32 years and must therefore be produced. To do so, tritium breeding blankets composed of lithium orthosilicate (Li_4SiO_4) are placed around the plasma chamber and fission annulus. Lithium occurs naturally in two isotopes: 7% is ^{6}Li and 93% is ^{7}Li. Tritium is therefore produced by the reactions

$$ {}_3^6\mathrm{Li}+{}_0^1n\rightarrow{}_1^3\mathrm{T}+{}_2^4\mathrm{He} \quad (1) $$

and

$$ {}_3^7\mathrm{Li}+{}_0^1n\rightarrow{}_1^3\mathrm{T}+{}_2^4\mathrm{He}+{}_0^1n\ . \quad (2) $$

Reaction (2) is endothermic with a threshold energy of $E_n = 2.466$ MeV, whereas reaction (1) is exothermic. This, combined with the high absorption cross section of ^{6}Li for neutrons at thermal energies, causes the ^{6}Li reaction to be far more effective at tritium production despite its much lower isotopic content. The lithium in the SABrR tritium breeding blankets is enriched to 93% ^{6}Li by weight to increase the tritium production rate.

II.C. Annular Fast Reactor

Each SABrR fuel assembly (Fig. 3) is a hexagonal duct measuring 15.5 cm across-flats.[12] The duct is filled with ten rings of fuel pins on a hexagonal lattice, for a total of 271 pins per assembly. The pins are separated by a wire wrap at a pitch of 8.9 mm. The fuel pins (Fig. 4) are based on the pins developed in the IFR initiative for S-PRISM (Ref. 18). The cladding is ODS MA957, a ferritic oxide dispersion strengthened (ODS) steel that is estimated to withstand up to 200 displacements per atom (DPA). ODS MA957 was developed as a low-swelling ferritic steel for fast reactor cladding; at low-temperature irradiation ($T < 355$°C), the ductile-to-brittle transformation temperature shifts upward significantly, causing embrittlement as a failure mode at relatively low accumulated radiation damage.[19,20] For this reason, the lowest cladding temperature in SABrR is $\sim$380°C and is located at the lower edge of the lower axial blanket, where the fast neutron fluence is significantly below average; similarly, the region of maximum fast fluence (at the core midplane) has cladding temperatures well in excess of 400°C. Around the cladding is a $LiNbO_3$ sheath that provides electrical insulation to prevent a large magneto-hydrodynamic pressure drop in the liquid metal coolant.

The fission core fuel height is 200 cm, but this is axially expanded to 210 cm in the computational model to account for thermal and irradiation-induced axial swelling of the fuel column, which occurs at very low burnup.[21–23] The densities are correspondingly adjusted downward to keep the fuel mass constant. An R-Z cross section of the fuel zones in the fission annulus is shown in Fig. 5. The driver fuel is located in the axially centered 150 cm of the second and third assembly rings. There are 30-cm axial blankets both above and below the driver fuel. Radial blanket assemblies occupy rings 1 and 4.

The driver fuel is a U-Pu-10Zr ternary alloy very similar to several of the pin compositions tested in EBR-II and the fast flux test facility.[21,24] The fuel slug has a smear density of 75% to allow for burnup-related swelling due to the production of gaseous fission products. These

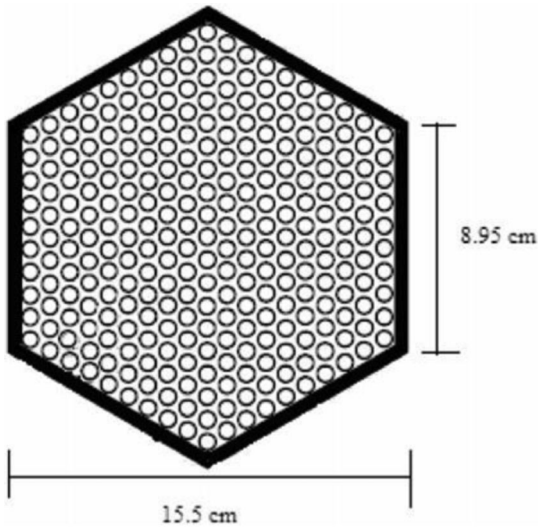

Fig. 3. SABrR fuel assembly.

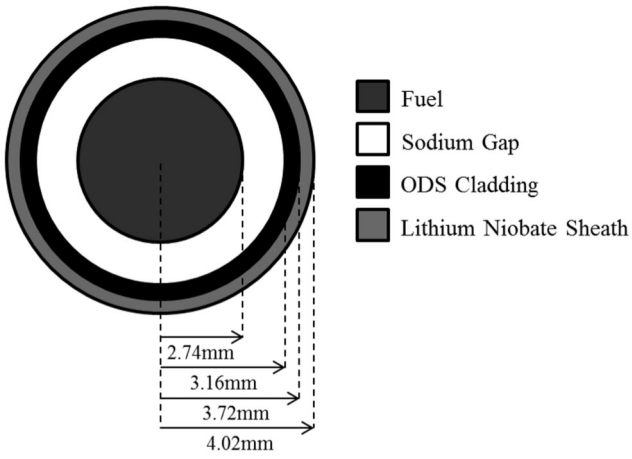

Fig. 4. SABrR fuel pin.

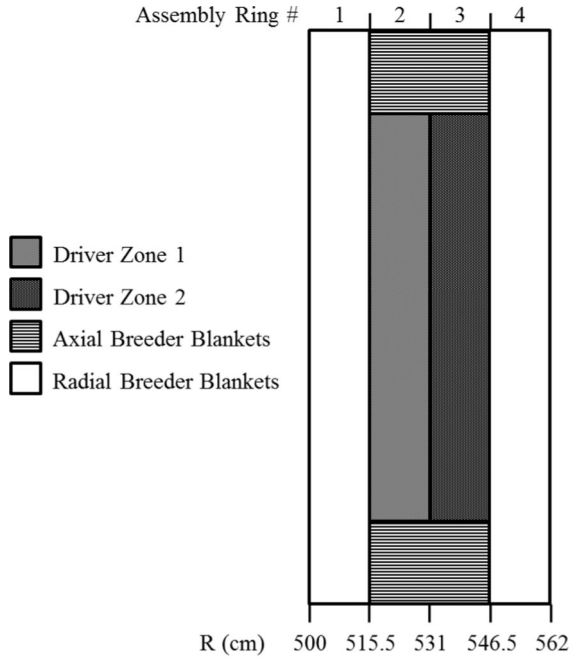

Fig. 5. SABrR fuel loading.

gases cause the fuel to become porous and swell radially until it contacts the cladding. At ~1% burnup, the porosity is high enough that the pores become interconnected and the fission gases are released to the plenum; further gaseous fission products that are produced do not contribute to further swelling, and thus, high burnups are achievable.[22,23] In some of the test pins in EBR-II, burnups of almost 20 at. % were demonstrated in several of the test pins without issue; these tests were ongoing when the reactor was shut down, so 20 at. % can be considered a lower limit of the burnup potential of that fuel. The plutonium vector of the driver fuel is given in Table I; it was developed for high-burnup metal fuels.[14] The plutonium enrichment in driver zone 2 (in the third assembly ring) is 23.75%, slightly higher than in driver zone 1, at 22.36%, to flatten the radial power profile, and it receives fewer fusion neutrons as it is farther away.

The radial blanket fuel is a U-10Zr alloy at 85% smear density; it is similar to the Mark-I fuel pins for EBR-II, except with 10% Zr by weight instead of 5% fissium (a description of fissium is given in Ref. 23). The ^{235}U enrichment is 0.25% by weight. The 10% Zr was chosen because of its beneficial effect on the fuel melting temperature and on fuel-cladding interactions. While the lower uranium volume fraction likely has a slightly negative effect on breeding, the plasma-side edge of the inner radial blanket receives the fusion neutrons most directly and thus has a relatively high power for a fast reactor blanket; therefore, the thermal considerations are of primary importance. For that same reason, the pin diameter and number of pins per assembly are kept the same as in the driver fuel rather than using the fewer, larger pins found in most blanket assembly designs. The Mark-II fuel pins were limited to 3 at. % burnup in EBR-II due to burnup-induced swelling; these pins are similarly limited.

The axial blankets are the same composition as the radial blankets, but at 75% smear density to allow the fission gases from the driver fuel easy access to the plenum. Because of their lower smear density, the burnup limit of the axial blankets matches that of the driver fuel.

The breeding of fissile material occurs by neutron capture in fertile isotopes within the fission annulus. The primary fertile isotope is ^{238}U, which captures a neutron and then decays by beta emission twice before becoming fissile ^{239}Pu:

$$^{238}_{92}\mathrm{U} + {}^{1}_{0}n \rightarrow {}^{239}_{92}\mathrm{U}^{*} \xrightarrow{\beta} {}^{239}_{93}\mathrm{Np} \xrightarrow{\beta} {}^{239}_{94}\mathrm{Pu}\ . \qquad (3)$$

The decay to ^{239}Np occurs with a half-life of 23 min, and the decay to ^{239}Pu has a half-life of 2.4 days; thus, ^{239}Np reaches near-steady-state levels very shortly after the beginning of the fuel residence. There are two fertile isotopes of Pu as well: ^{238}Pu and ^{240}Pu. Each of these can capture a neutron to become ^{239}Pu and ^{241}Pu, respectively:

TABLE I

Plutonium Vector of Driver Fuel

Isotope	Weight Percent
^{238}Pu	2.102
^{239}Pu	58.258
^{240}Pu	25.976
^{241}Pu	9.76
^{242}Pu	3.904

$$^{238}_{94}\mathrm{Pu} + ^{1}_{0}n \rightarrow ^{239}_{94}\mathrm{Pu} \quad (4)$$

and

$$^{240}_{94}\mathrm{Pu} + ^{1}_{0}n \rightarrow ^{241}_{94}\mathrm{Pu} \; . \quad (5)$$

Because ^{238}U is the most common isotope of the three in the fresh driver fuel, most of the fissile production is through the first reaction, though all three substantially contribute. In the blanket assemblies, only ^{238}U is initially present, so nearly all fissile production there occurs via ^{239}Np.

III. COMPUTATIONAL MODEL

III.A. Calculation Methodology

SABrR was modeled in ERANOS (European Reactor ANalysis Optimized calculation System)[25], a fast reactor code system developed to model the Phénix and SuperPhénix reactors. ERANOS employs the European Cell COde (ECCO) to collapse 1968-group JEFF2.0 cross sections within each reactor lattice cell to the 33 groups used in core calculations, ranging from 20 MeV down to 0.1 eV. The core geometry was described in R-Z cylindrical geometry and the core calculations performed in the ERANOS discrete ordinates transport module BISTRO using an S8 quadrature with 132 radial and 216 axial mesh points. The fuel was depleted for 100 days in each burnup step in the EVOLUTION module before reperforming the core neutron flux calculations.

At each depletion step, the neutron source multiplication k_{mult} is calculated, and the neutron source strength is adjusted such that the fission annulus output is 3000 MW(thermal). The fusion power P_{fus} required to maintain a given fission power P_{fis} is determined by k_{mult}, the average number of neutrons released per fission ν, the energy released per fusion E_{fus}, and the energy released per fission E_{fis}:

$$P_{fus} = P_{fis}\left(\frac{1-k_{mult}}{k_{mult}}\right)\nu\left(\frac{E_{fus}}{E_{fis}}\right) \; . \quad (6)$$

It is important to note that k_{mult} differs from the more familiar k_{eff}. The TBR is also calculated at each step to determine if enough tritium is being produced to fuel sustained operation of the fusion neutron source. The TBR is defined as

$$\mathrm{TBR}(t) = \frac{\int_V \Sigma_c^{\mathrm{Li}}\phi(\mathbf{r},t)dV}{\int_V S(\mathbf{r},t)dV} \; , \quad (7)$$

where S is the fusion neutron source. This only accounts for production of T by ^{6}Li capture and thus is a conservative estimate of the TBR, as T produced in the threshold reaction in ^{7}Li is not counted in the ERANOS calculation. However, since the tritium breeding material is highly enriched in ^{6}Li and the cross section for production via that route is much higher, the approximation should be quite close to the true tritium production rate.

The FBR is the instantaneous ratio of the production rate of fissile atoms to their destruction rate, whether through fission or parasitic capture:

$$\mathrm{FBR}(t) = \frac{P(t)}{D(t)} \; . \quad (8)$$

The production rate is calculated by integrating the capture rates of the fertile isotopes over the reactor volume:

$$P(t) = \int_V \left(\Sigma_c^{^{238}\mathrm{U}}(\mathbf{r})\phi(\mathbf{r},t) + \Sigma_c^{^{238}\mathrm{Pu}}(\mathbf{r})\phi(\mathbf{r},t) + \Sigma_c^{^{240}\mathrm{Pu}}(\mathbf{r})\phi(\mathbf{r},t)\right)dV \; . \quad (9)$$

Though ^{239}Np, rather than ^{238}U, is technically the precursor to ^{239}Pu, ^{239}Np exists in the reactor in a near steady state after its first few half-lives. Thus, by approximately day 20 of fuel residence time, the decay rate of ^{239}Np is equal to the capture rate of ^{238}U. The destruction rate is the volume-integrated absorption rate for all of the fissile isotopes. Only ^{235}U, ^{239}Pu, and ^{241}Pu exist in substantial amounts in the reactor, so other fissile isotopes are omitted from the summation:

$$D(t) = \int_V \left(\Sigma_{abs}^{^{235}\mathrm{U}}(\mathbf{r})\phi(\mathbf{r},t) + \Sigma_{abs}^{^{239}\mathrm{Pu}}(\mathbf{r})\phi(\mathbf{r},t) + \Sigma_{abs}^{^{241}\mathrm{Pu}}(\mathbf{r})\phi(\mathbf{r},t)\right)dV \; . \quad (10)$$

Substituting these expressions for the production and destruction rates into Eq. (8), we have

$$\mathrm{FBR}(t) = \frac{P(t)}{D(t)} = \frac{\int_V \left(\Sigma_c^{^{238}\mathrm{U}}(\mathbf{r})\phi(\mathbf{r},t) + \Sigma_c^{^{238}\mathrm{Pu}}(\mathbf{r})\phi(\mathbf{r},t) + \Sigma_c^{^{240}\mathrm{Pu}}(\mathbf{r})\phi(\mathbf{r},t)\right)dV}{\int_V \left(\Sigma_{abs}^{^{235}\mathrm{U}}(\mathbf{r})\phi(\mathbf{r},t) + \Sigma_{abs}^{^{239}\mathrm{Pu}}(\mathbf{r})\phi(\mathbf{r},t) + \Sigma_{abs}^{^{241}\mathrm{Pu}}(\mathbf{r})\phi(\mathbf{r},t)\right)dV} \; . \quad (11)$$

III.B. Design Constraints

There were four hard constraints placed on the reactor design that, if violated, were a termination point for that particular case. First, the TBR must not fall below 1.15. This value was chosen because tritium self-sufficiency is a requirement for sustained fusion operation and previous calculations indicate that this excess above unity allows for losses due to inefficiency in tritium collection and for the radioactive decay of any tritium in inventory throughout the operating and refueling cycles. Second, the radiation damage limit of the clad must not be exceeded. The damage limit of ODS MA957 in a fission spectrum is estimated at either 200 DPA or at an accumulated fast fluence of 4×10^{23} n/cm^2. Third, no blanket zone may surpass 3 at. % burnup, as per the EBR-II Mark-II fuel pin tests. Fourth, no driver fuel may exceed 13.33 at. % burnup; this is reduced from the 20 at. % reached in the IFR pin tests because whereas most fast reactor fuel pins have a plenum-to-fuel volume ratio of unity, the SABrR pins have a ratio of only 2/3.

There were also soft constraints placed on each case, which were considered more as design guidelines. If a soft constraint is violated, the scenario may be continued either if the violation is temporary or if a scenario is approaching the violation of a hard constraint. There were two soft constraints. First, k_{eff} should be significantly below 1 ($k_{eff} < 0.95$ was desired), such that $|\rho| \gg \beta$, and the reactor is always very far from prompt critical. Second, the output of the fission core plus blankets should be maintained at 3000 MW(thermal) using a maximum of 500 MW of fusion power, the ITER design power level.

IV. RESULTS AND DISCUSSION

IV.A. TBR Case

The configuration of reflector and tritium breeding blanket that emphasizes a high TBR is shown in relation to the fission core and plasma in Fig. 6. Placing the outboard tritium breeding blanket adjacent to the fission annulus results in a higher neutron capture rate in the blanket than if it were located radially outside the reflector. However, the increase in neutron capture comes at the expense of some of the fissile breeding in the outer radial fissile blanket.

The k_{eff}, k_{mult}, and fusion power required to drive the fission annulus at 3000 MW(thermal) are shown in Fig. 7. Shortly before reaching 2000 days of fuel residence time, the fusion power exceeds 500 MW, but the blanket fuel in the plasma-side edge of the inner radial blanket reaches 3% burnup soon after day 2300, at a fusion power of 513 MW. The maximum burnup in the driver fuel is 9.31%, well below its burnup limit of 13.33%. The TBR is substantially above 1.15 for the entire cycle, and the FBR is 1.299 at its peak and 1.278 at the end of the fuel residence time. The average net fissile production over the residence time is 208.4 kg/year.

The fast fluence ($E_n > 0.1$ MeV) and DPA accumulation in the cladding across the fission core midplane are shown in Fig. 8 at various points throughout the fuel life; the end of cycle (EoC) is after 2300 days. The contribution of the 14.1-MeV fusion neutrons to the total radiation damage can be seen in the upturn of the DPA curve near $R = 500$ cm. Because these

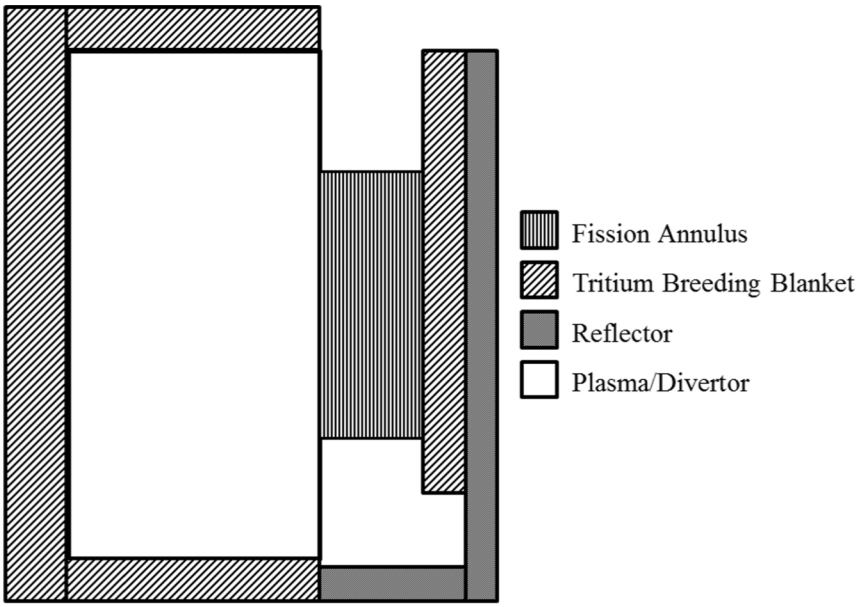

Fig. 6. Configuration favoring TBR (other reactor structures omitted).

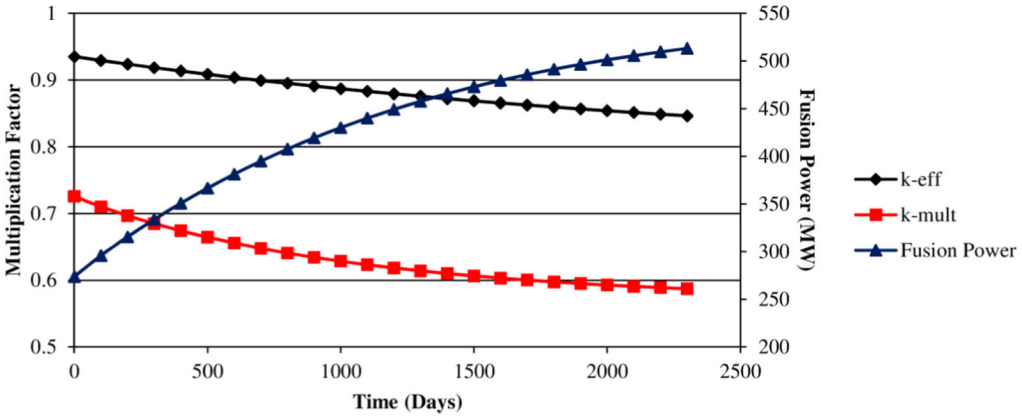

Fig. 7. Multiplication values and fusion power for TBR case.

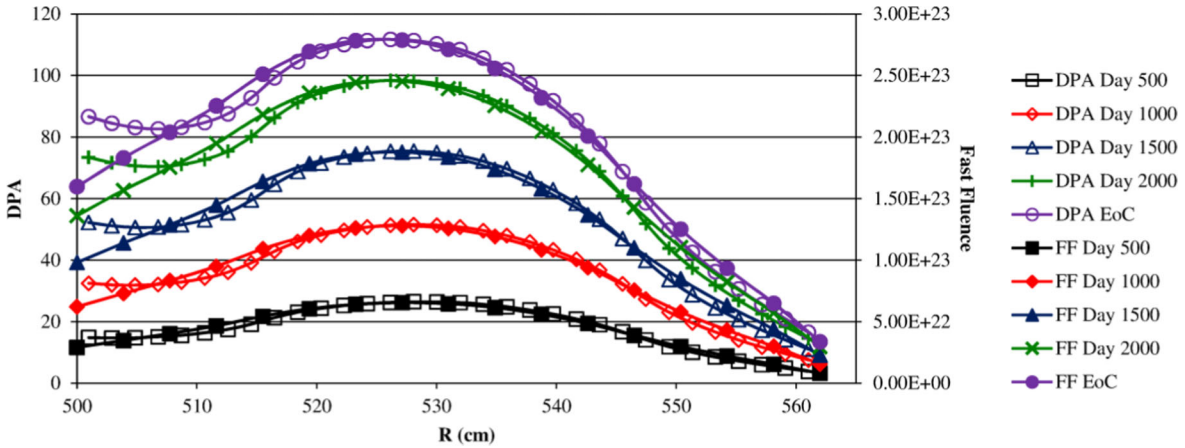

Fig. 8. Accumulated DPA and fast fluence across core midplane in TBR configuration.

unmoderated fusion neutrons are far more damaging than the average fission neutron in the core, while the fast fluence tallies all neutrons above 0.1 MeV equally, the two curves diverge at the plasma source despite their agreement throughout the rest of the core. This difference is more pronounced later in the core residence time when the source power has been turned up, but the peak for both measures of radiation damage still lies near the midpoint of the fission core and is well below the design limits.

IV.B. FBR Case

The configuration of reflector and tritium breeding blanket that emphasizes a higher FBR is shown in relation to the plasma and fission core in Fig. 9.

The k_{eff}, k_{mult}, and fusion power required to drive 3000 MW(thermal) in the FBR case are shown in Fig. 10. The higher multiplication values and the lower fission power are due to fewer net neutrons leaking radially outward from the outer radial blanket zone than in the case favoring the TBR. This directly causes both more power and more fissile production in that assembly ring and indirectly increases those values in the adjacent driver fuel. The limiting factor for fuel residence time in this configuration is, as in the TBR case, the burnup limit of the plasma-edge blanket fuel being reached. However, because of the relatively lower fusion power throughout the entire residence time and the consequently lower contribution to the 3000-MW(thermal) fission output from that zone, it took 2600 days to reach the limit. The driver fuel has a maximum burnup of 10.23%, comfortably below its maximum. The TBR, while lower in this case than in the case favoring tritium production, is 1.206 at its lowest (this occurs at the EoC), with most of the difference resulting from decreased production in the outboard tritium breeding blanket. The FBR is 1.34 at its peak and 1.298 at the EoC. An average net of 253.7 kg/year of fissile material is produced each year in this configuration.

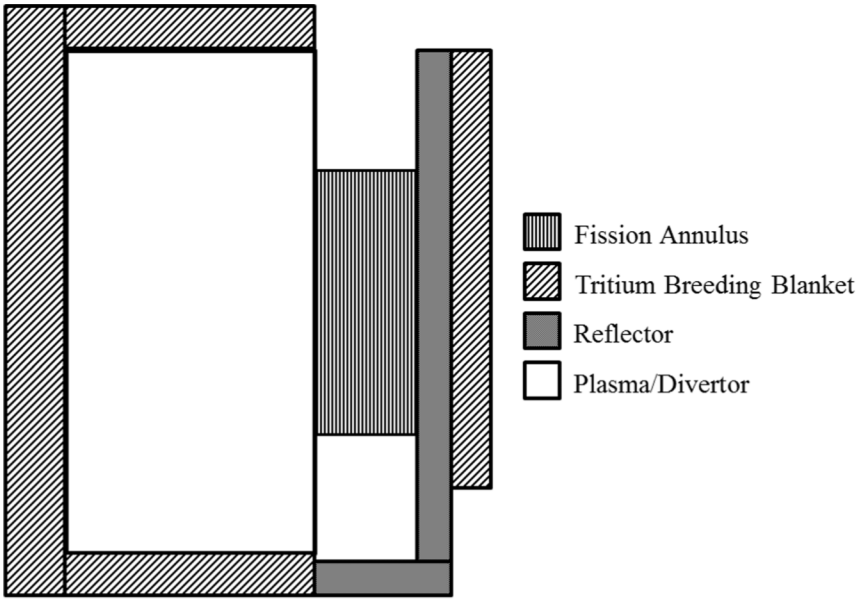

Fig. 9. Configuration favoring FBR (other reactor structures omitted).

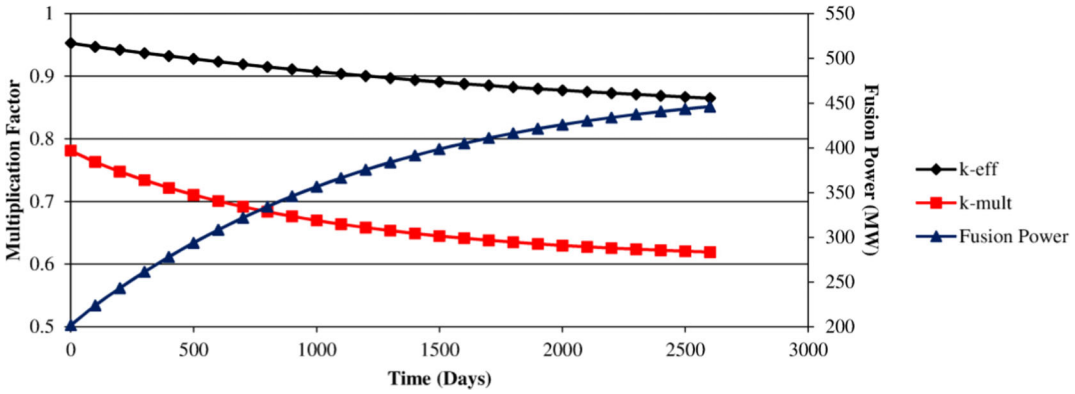

Fig. 10. Multiplication values and fusion power for FBR case.

The fast fluence and DPA accumulation across the core midplane are shown in Fig. 11 at various points throughout the fuel life; the EoC occurs after 2600 days. Similarly to the TBR case, the fusion neutrons cause a divergence of the DPA and fast fluence near the plasma, but the peaks of both curves are near the annulus center. The maximum DPA is 124, and the maximum fast fluence is 3.12×10^{23} n/cm^2.

IV.C. Neutronic Effect of Insulating Sheath

A sensitivity study was performed on the FBR configuration to evaluate the effects of removing the $LiNbO_3$ insulating sheath from around each fuel pin. The motivation for doing so stems from the desire to compare with critical fast breeder reactors, which do not require the insulator. While oxide-fueled reactors will have oxygen present in greater fractional quantities than SABrR, Li is absent in even those cores and represents a moderating element unique to SABrR. Though the insulating sheath is less dense than the cladding, it occupies 9.5% of the cross-sectional area within each fuel assembly, so its effect is nonnegligible.

For this study, the reactor geometry is otherwise identical to the FBR configuration, and the enrichment of the driver fuel is kept the same. Because the base FBR configuration was able to run until day 2600 before violating one of the design constraints, the sensitivity study was

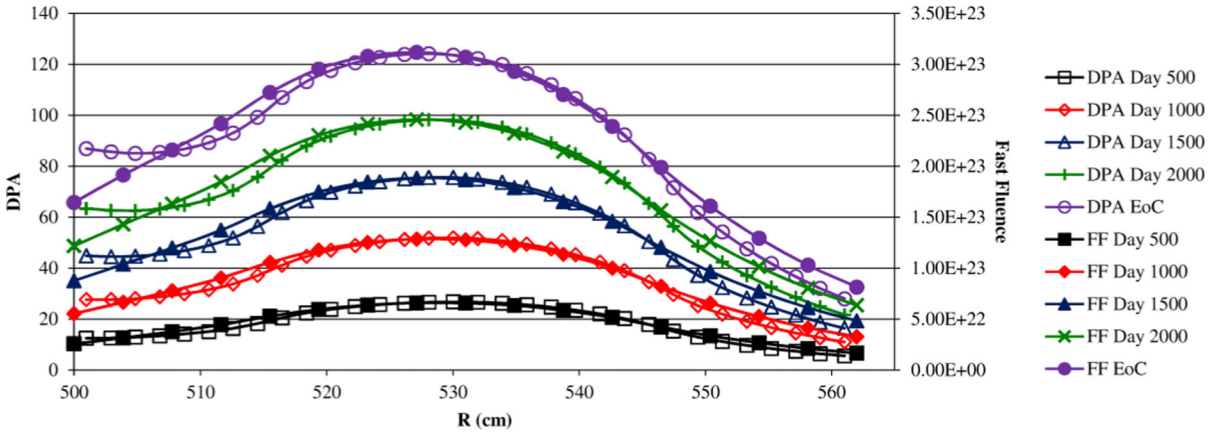

Fig. 11. Accumulated DPA and fast fluence across core midplane in FBR configuration.

carried out for the same duration, regardless of violation of design constraints. The effects of removing the sheath from around the fuel pins are summarized in Table II.

The removal of the sheath hardened the neutron spectrum (Fig. 12). The fission-to-capture ratios of the fuel consequently rose, resulting in a more reactive fission annulus that was easier to drive with the neutron source. The higher fission-to-capture ratios of the fissile isotopes meant a lower destruction rate for a given fission power, which increases the FBR; however, this effect was outcompeted by the increase in leakage from the fission annulus, so the resulting FBR is slightly lower due to reduced capture in fertile isotopes. This increase in leakage from the fission annulus is also evident in the higher TBR. Though the demand on the fusion neutron source, and thus the tritium destruction rate, is lower without the sheath, the majority of the tritium production occurs in the blankets surrounding the plasma, whose production is highly dependent on the neutron source strength.

IV.D. Neutron Spectra Comparison

The neutron spectra at several points in the core for the TBR and FBR cases are shown in Figs. 13 and 14, respectively, at 1000 days into the fuel residence time; the spectrum in the inner radial blanket only 2 cm away from the plasma demonstrates the effect of the neutron source on the overall spectrum. The spectra are similar throughout the fission annulus; however, in the outboard tritium breeding blanket, there is a pronounced softening of the spectrum. The presence of the reflector between the fission annulus and the tritium breeding blanket in the FBR case significantly enhances this softening of the spectrum relative to the TBR case.

IV.E. Power Distributions

The distribution of power produced in the driver and in the fission blankets changes significantly as burnup

TABLE II

Effects of Removing Insulating Sheath

Quantity	FBR Configuration Base Case	$LiNbO_3$ Sheath Removed
BoC k_{eff}[a]	0.953	0.971
EoC k_{eff}	0.865	0.879
BoC k_{mult}	0.781	0.870
EoC k_{mult}	0.619	0.666
BoC P_{fus} (MW)	202	108
EoC P_{fus} (MW)	446	364
FBR (peak/EoC)	1.34/1.298	1.301/1.277
Fissile gain (kg/year)	253.7	212.4
TBR (minimum)	1.206	1.366
Peak blanket burnup (at. %)	2.98	2.43
Peak driver burnup (at. %)	10.23	10.48

[a]BoC = beginning of cycle.

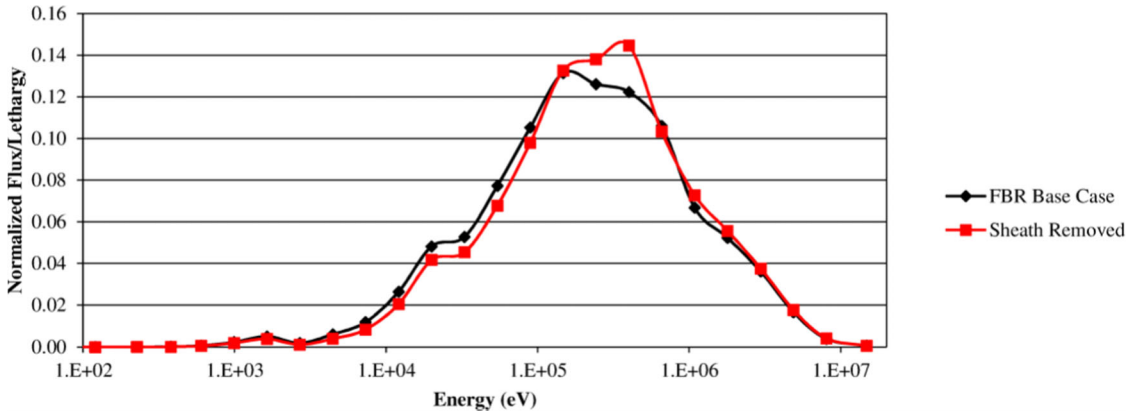

Fig. 12. Neutron (core-center) spectrum comparison of sheathed and unsheathed pins.

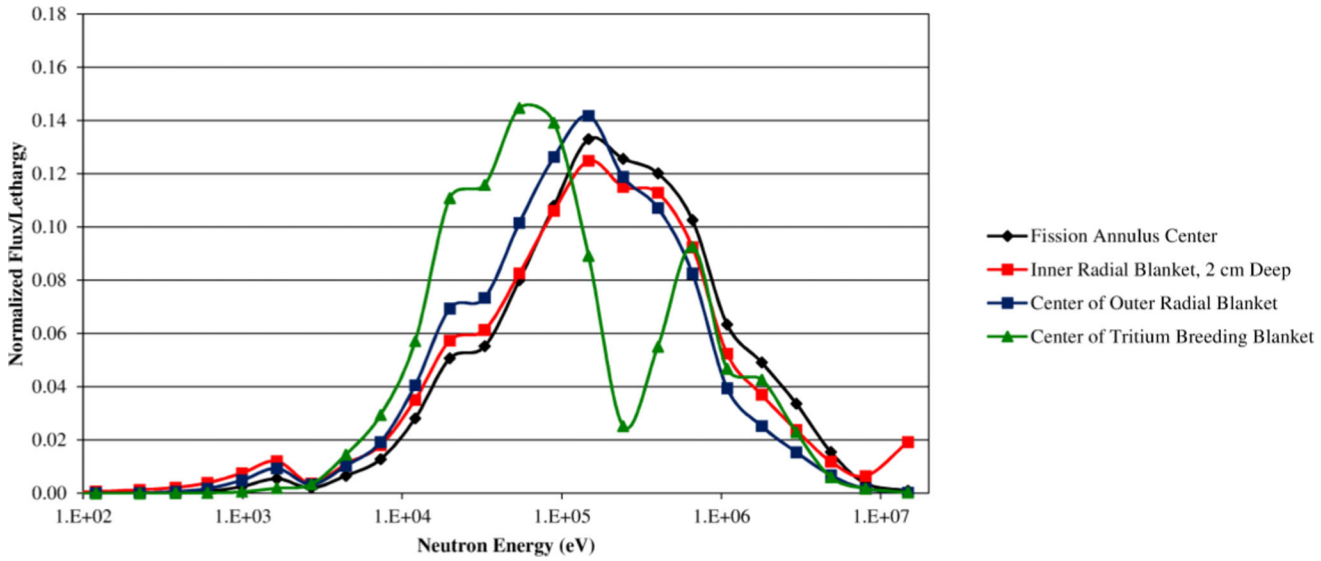

Fig. 13. Neutron spectra at 1000 days at selected locations (TBR case).

progresses. Initially, the driver fuel produces nearly all of the fission power, but as fissile isotopes are depleted from the driver fuel and bred in the blankets, the blankets produce an increasing fraction of the power. This increase in blanket power is more pronounced in the inner radial blanket assemblies than the outer ones, as they are exposed directly to the fusion neutron source and thus have a higher rate of breeding and a high incident neutron flux from the plasma. The radial power distribution for the FBR case is shown for various times in the burnup cycle in Fig. 15.

The TBR case power distribution is almost identical to that of the FBR case. The power at any given time in the burnup cycle is slightly higher in the inner radial blanket than in the FBR due to the comparatively higher incident fusion neutron flux. The outer radial blanket power is slightly lower in the TBR case due to competing neutron capture in the adjacent tritium breeding blanket suppressing fissile production and reducing the neutron flux in that region.

IV.F. Comparison to Critical Fast Reactor System

A comparison of the breeding performance of SABrR with the high-breeding metal-fueled S-PRISM core design[18] from which the SABrR fuel pins were adapted is shown in Table III. This critical system was chosen for the comparison because of the pin similarity and because of the maturity of the S-PRISM design.

The lower specific power and higher TRU loading of SABrR are a direct consequence of the annular geometry of its fission core; such geometry has a much higher leakage than the traditional pancaked cylinder, so the driver fuel k_∞ must be correspondingly higher, even for

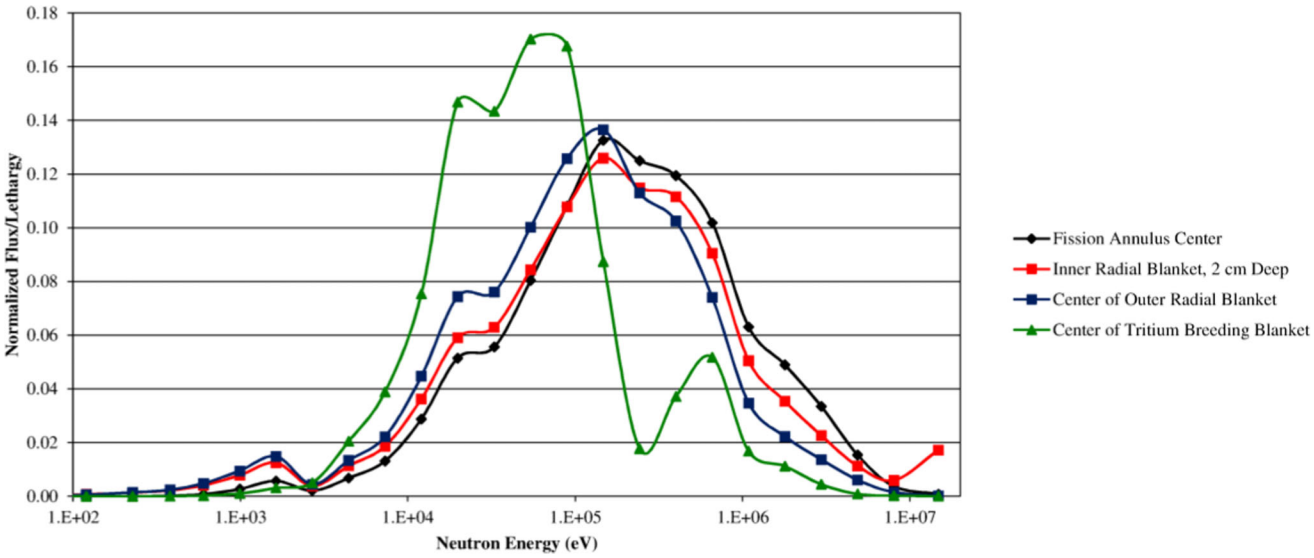

Fig. 14. Neutron spectra at 1000 days at selected locations (FBR case).

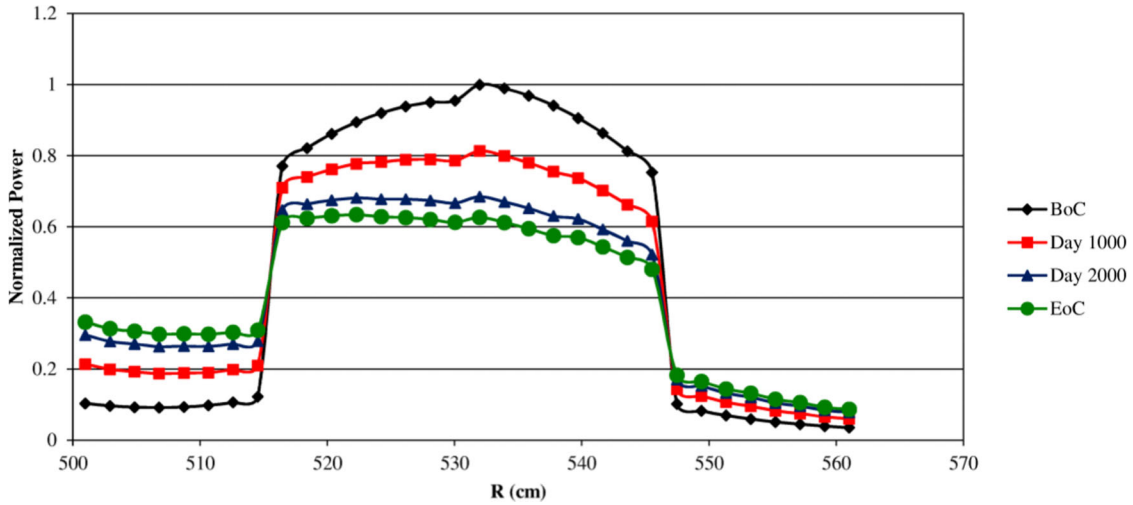

Fig. 15. Radial power distribution across centerline of the fission annulus at various residence times (FBR case).

a lower k_{eff}. The higher fissile loading of SABrR means that despite its higher FBR, it has a longer doubling time. However, the fissile gain normalized to fission core thermal power is roughly equal for the SABrR TBR case and S-PRISM, while the SABrR FBR case exceeds S-PRISM in this regard.

SABrR has a higher fuel residence duration than the driver fuel of S-PRISM but a slightly lower blanket residence time. This S-PRISM core design is radially heterogeneous and utilizes blanket shuffling to flatten the radial power profile. SABrR, however, does not shuffle assemblies at any point during the burnup cycle; the presence of the neutron source at the edge of the fission annulus and the ability to adjust its strength largely negate the need to do so for power flattening purposes. Therefore, SABrR would be shut down far less frequently for shuffling/refueling purposes, which is an advantage it holds over nearly all critical systems.

Because cycle length for both the FBR and TBR cases for SABrR were limited by blanket burnup in ring 1 with a reasonable margin to peak radiation damage and driver burnup limits, the radial blankets in rings 1 and 4 might be switched midcycle to increase total residence time, although at the cost of increased downtime. Finding a suitable electrically insulating material that has less moderating power than the $LiNbO_3$ would also extend the cycle duration of SABrR since the blanket burnup limit was not reached in that scenario. A less-moderating

TABLE III

Breeding Performance Comparison of SABrR to S-PRISM

Quantity	SABrR			S-PRISM
Core thermal power (MW)	3 000			1 000
BoC Pu loading (kg)[a]	14 317.0			3 159.9
BoC fissile Pu loading (kg)	9 738.2			2 458.8
BoC U loading (kg)	164 763.1			33 052.7
Specific power (W/g Pu)	209.54			316.47
Pu enrichment [wt%, Pu/(U + Pu)]	Driver zone 1: 22.36 Driver zone 2: 23.75			21.29
	TBR Case	FBR Case	Unsheathed	—
Fuel residence time (days)	2300	2600	2600	Driver: 2070 Blanket: 2760
Cycle-average breeding ratio	1.28	1.32	1.28	1.22
Fissile gain (kg/year)	208.39	253.73	212.37	69.91
Normalized fissile gain [kg/(MW(thermal)·year]	0.0695	0.0846	0.0708	0.0699

[a]BoC = beginning of cycle.

insulator would allow for either decreased fissile enrichment of the driver fuel or for radially heterogeneous core layouts, which do not increase driver enrichment to high levels.

We note that no attempt has been made to optimize these initial SABrR designs for fissile production within a particular fuel cycle. In principle, subcritical operation (a) removes the criticality requirement, which allows the fuel and blanket to remain in the reactor until the clad radiation damage limit is reached, and (b) increases the reactivity margin to prompt critical by an order of magnitude, which removes any safety limitation on Pu content in the reactor. A future investigation will seek to leverage these two factors to improve the fissile production performance of SABrR for comparison against critical fast burner reactors. Our purpose in this paper was to investigate whether the SABR burner reactor concept (technology, geometry, and major parameters) could be adapted to a breeder reactor that had a reasonable fissile production performance.

V. CONCLUSION

The SABR FFH fast burner reactor configuration, based on IFR-PRISM fast reactor physics and technology and on ITER fusion physics and technology, was investigated for a fast breeder reactor application. Representative configurations for breeding fissile material from depleted uranium while simultaneously breeding tritium were considered, subject to realistic constraints on (a) the radiation damage to the cladding (200 DPA or 4×10^{23} n/cm^2 fast fluence), (b) driver fuel burnup (13.33 at. %), (c) blanket fuel burnup (3 at. %), and (d) TBR (> 1.15). The representative designs considered were found to be capable of producing FBRs ~ 1.3 and maintaining TBRs > 1.2. This neutron economy is sufficient to produce ~ 250 kg/year of fissile material in a 3000-MW(thermal) plant while also producing enough tritium for self-sufficiency of the fusion neutron source fuel.

While this study demonstrates the capability of the SABrR FFH fast breeder concept to breed significant excess fissile material, it has not addressed the issue of any possible safety advantage of a FFH breeder relative to a similar critical breeder, and this should be done as a next step in this line of investigation.

ACKNOWLEDGMENTS

This research is being performed using funding received from the U.S. Department of Energy Office of Nuclear Energy's Nuclear Energy University Programs.

REFERENCES

1. R. D. VAUGHAN, "Uranium Conservation and the Role of the Gas Cooled Fast Breeder Reactor," *J. Br. Nucl. Energy Soc.*, **14**, 105 (1975).

2. G. A. VENDRYES, "Superphénix: A Full-Scale Breeder Reactor," *Sci. Am.*, **236**, 26 (1977); http://dx.doi.org/10.1038/scientificamerican0377-26.

3. Y. I. CHANG et al., "Advanced Burner Test Reactor Preconceptual Design Report," ANL-ABR-1, Argonne National Laboratory (2008).

4. E. A. HOFFMAN, W. S. YANG, and R. N. HILL, "Preliminary Core Design Studies for the Advanced Burner Reactor over a Wide Range of Conversion Ratios," ANL-AFCI-177, Argonne National Laboratory (2008).

5. A. ROMANO, P. HEJZLAR, and N. E. TODREAS, "Fertile-Free Fast Lead-Cooled Incinerators for Efficient Actinide Burning," *Nucl. Technol.*, **147**, 368 (2004); http://dx.doi.org/10.13182/NT04-1.

6. C. E. TILL, Y. I. CHANG, and W. H. HANNUM, "The Integral Fast Reactor—An Overview," *Prog. Nucl. Energy*, **31**, 3 (1997); http://dx.doi.org/10.1016/0149-1970(96)00001-7.

7. C. E. TILL and Y. I. CHANG, "Plentiful Energy: The Story of the Integral Fast Reactor," CreateSpace (2011).

8. H. CHOI and A. BAXTER, "A Comparative Study on Recycling Spent Fuels in Gas-Cooled Fast Reactors," *Ann. Nucl. Energy*, **37**, 723 (2010); http://dx.doi.org/10.1016/j.anucene.2010.01.014.

9. S. PIET et al., "Which Elements Should Be Recycled for a Comprehensive Fuel Cycle?" *Proc. Global 2007 Advanced Nuclear Fuel Cycle and Systems*, Boise, Idaho, September 2007, Idaho National Laboratory; see also INL/CON-07-12197: www.osti.gov/scitech/biblio/920405 (current as of May 2014).

10. R. N. HILL et al., "Multiple Tier Fuel Cycle Studies for Waste Transmutation," *Proc. 10th Int. Conf. Nuclear Engineering (ICONE 10)*, Arlington, Virginia, April 14–18, 2002.

11. J. P. ACKERMAN et al., "Treatment of Wastes in the IFR Fuel Cycle," *Prog. Nucl. Energy*, **31**, 141 (1997); http://dx.doi.org/10.1016/0149-1970(96)00008-X.

12. W. M. STACEY et al., "A TRU-Zr Metal-Fuel Sodium-Cooled Fast Subcritical Advanced Burner Reactor," *Nucl. Technol.*, **162**, 53 (2008); http://dx.doi.org/10.13182/NT08-1.

13. W. M. STACEY, "Principles and Rationale of the Fusion-Fission Hybrid Burner Reactor," *AIP Conf. Proc.*, **1442**, 31 (2012).

14. C. M. SOMMER, W. M. STACEY, and B. PETROVIC, "Fuel Cycle Analysis of the SABR Subcritical Transmutation Reactor Concept," *Nucl. Technol.*, **172**, 48 (2010); http://dx.doi.org/10.13182/NT10-3.

15. C. M. SOMMER et al., "Transmutation Fuel Cycle Analyses of the SABR Fission-Fusion Hybrid Burner Reactor for Transuranic and Minor Actinide Fuels," *Nucl. Technol.*, **182**, 274 (2013); http://dx.doi.org/10.13182/NT11-55.

16. R. W. MOIR, "The Fusion Breeder," *J. Fusion Energy*, **2**, 351 (1982); http://dx.doi.org/10.1007/BF01063686.

17. R. W. MOIR et al., "Fusion Breeder Reactor Design Studies," *Nucl. Technol./Fusion*, **4**, *4*, part 2, p. 589 (1983).

18. A. E. DUBBERLEY et al., "Super-PRISM Oxide and Metal Fuel Core Designs," *Proc. 8th Int. Conf. Nuclear Engineering (ICONE 8)*, Baltimore, Maryland, April 2–6, 2000.

19. B. VAN DER SHAAF et al., "High Dose, up to 80 DPA, Mechanical Properties of Eurofer 97," *J. Nucl. Mater.*, **386–388**, 236 (2009); http://dx.doi.org/10.1016/j.jnucmat.2008.12.329.

20. A. ALAMO et al., "Mechanical Properties of 9Cr Martensitic Steels and ODS-FeCr Alloys After Neutron Irradiation at 325°C up to 42 DPA," *J. Nucl. Mater.*, **367–370**, 54 (2007); http://dx.doi.org/10.1016/j.jnucmat.2007.03.166.

21. A. L. PITNER and R. B. BAKER, "Metal Fuel Test Program in the FFTF," *J. Nucl. Mater.*, **204**, 124 (1993); http://dx.doi.org/10.1016/0022-3115(93)90208-G.

22. R. G. PAHL et al., "Experimental Studies of U-Pu-Zr Fast Reactor Fuel Pins in the Experimental Breeder Reactor-II," *Metall. Trans. A*, **21A**, 1863 (1990); http://dx.doi.org/10.1007/BF02647233.

23. R. G. PAHL et al., "Irradiation Behavior of Metallic Fast Reactor Fuels," *J. Nucl. Mater.*, **188**, 3 (1992); http://dx.doi.org/10.1016/0022-3115(92)90447-S.

24. Y. I. CHANG, "Technical Rationale for Metal Fuel in Fast Reactors," *Nucl. Eng. Technol.*, **39**, 161 (2007); http://dx.doi.org/10.5516/NET.2007.39.3.161.

25. G. RIMPAULT et al., "The ERANOS Code and Data-System for Fast Reactor Analyses," *Proc. Int. Conf. New Frontiers of Nuclear Technology: Reactor Physics, Safety and High-Performance Computing (PHYSOR 2002)*, Seoul, Korea, October 7–10, 2002, American Nuclear Society (2002).